

References and Notes

1. L. E. Reichl, *The Transition to Chaos in Conservative Classical Systems: Quantum Manifestations* (Springer-Verlag, New York, 1992).
2. M. J. Davis, E. J. Heller, *J. Chem. Phys.* **75**, 246 (1981).
3. W. A. Lin, L. E. Ballentine, *Phys. Rev. Lett.* **65**, 2927 (1990).
4. A. Peres, *Phys. Rev. Lett.* **67**, 158 (1991).
5. J. Plata, J. M. Gomez-Llorente, *J. Phys. A* **25**, L303 (1992).
6. R. Utermann, T. Dittrich, P. Hänggi, *Phys. Rev. E* **49**, 273 (1994).
7. O. Bohigas, S. Tomsovic, D. Ullmo, *Phys. Rep.* **223**, 43 (1993).
8. S. Tomsovic, D. Ullmo, *Phys. Rev. E* **50**, 145 (1994).
9. S. D. Frisch, E. Doron, *Phys. Rev. E* **57**, 1421 (1998).
10. A. Mouchet, C. Miniatura, R. Kaiser, B. Grémaud, D. Delande, *Phys. Rev. E*, in press (available at xxx.lanl.gov/abs/nlin.CD/0012013).
11. W. K. Hensinger, A. G. Truscott, B. Upcroft, N. R. Heckenberg, H. Rubinsztein-Dunlop, *J. Opt. B Quant. Semiclass. Opt.* **2**, 659 (2000).
12. M. Hug, G. J. Milburn, *Phys. Rev. A* **63**, 023413 (2001).
13. S. Dyrting, G. J. Milburn, C. A. Holmes, *Phys. Rev. E* **48**, 969 (1993).
14. V. Averbukh, N. Moiseyev, B. Mirbach, H. J. Korsch, *Z. Phys. D* **35**, 247 (1995).
15. C. Dembowski et al., *Phys. Rev. Lett.* **84**, 867 (2000).
16. B. V. Chirikov, D. L. Shepelyansky, *Phys. Rev. Lett.* **74**, 518 (1995).
17. T. Neicu, K. Schaadt, A. Kudrolli, *Phys. Rev. E* **63**, 026206 (2001).
18. P. M. Koch, L. Sirko, R. Blümel, personal communication.
19. D. L. Haycock, P. M. Alsing, I. H. Deutsch, J. Grondalski, P. S. Jessen, *Phys. Rev. Lett.* **85**, 3365 (2000).
20. S. Ghose, P. M. Alsing, I. H. Deutsch, preprint available at xxx.lanl.gov/abs/quant-ph/0102085.
21. R. Graham, M. Schlautmann, P. Zoller, *Phys. Rev. A* **45**, R19 (1992).
22. D. A. Steck, V. Milner, W. H. Oskay, M. G. Raizen, *Phys. Rev. E* **62**, 3461 (2000).
23. J. C. Robinson et al., *Phys. Rev. Lett.* **76**, 3304 (1996).
24. M. T. DePue, C. McCormick, S. L. Winoto, S. Oliver, D. S. Weiss, *Phys. Rev. Lett.* **82**, 2262 (1999).
25. M. A. Kasevich, thesis, Stanford University, Stanford, CA (1992).
26. For an animation of this data (Fig. 1, C and D), see the supplementary material (36).
27. P. J. Martin, B. G. Oldaker, A. H. Miklich, D. E. Pritchard, *Phys. Rev. Lett.* **60**, 515 (1988).
28. D. M. Giltner, R. W. McGowan, S. A. Lee, *Phys. Rev. A* **52**, 3966 (1995).
29. M. Kozuma et al., *Phys. Rev. Lett.* **82**, 871 (1999).
30. G. Casati, R. Graham, I. Guarneri, F. M. Izrailev, *Phys. Lett. A* **190**, 159 (1994).
31. S. Tomsovic, *J. Phys. A* **31**, 9469 (1998).
32. For tunneling data with different Raman-selected velocity widths, see the supplementary material (36).
33. E. J. Heller, *J. Phys. Chem. A* **103**, 10433 (1999).
34. For animations of the data and phase space in Fig. 5, see the supplementary material (36).
35. W. K. Hensinger et al., *Nature*, in press.
36. The supplementary material is available at Science Online at www.sciencemag.org/cgi/content/full/1061569.
37. This work was supported by the NSF, the R. A. Welch Foundation, the Sid W. Richardson Foundation, and a Fannie and John Hertz Foundation Fellowship (D.A.S.). D.A.S. acknowledges fruitful discussions with K. W. Madison.

12 April 2001; accepted 1 June 2001  
 Published online 5 July 2001;  
 10.1126/science.1061569  
 Include this information when citing this paper.

# Deterministic Delivery of a Single Atom

Stefan Kuhr,\* Wolfgang Alt, Dominik Schrader, Martin Müller, Victor Gomer, Dieter Meschede

We report the realization of a deterministic source of single atoms. A standing-wave dipole trap is loaded with one or any desired number of cold cesium atoms from a magneto-optical trap. By controlling the motion of the standing wave, we adiabatically transport the atom with submicrometer precision over macroscopic distances on the order of a centimeter. The displaced atom is observed directly in the dipole trap by fluorescence detection. The trapping field can also be accelerated to eject a single atom into free flight with well-defined velocities.

The manipulation of individual atomic particles is a key factor in the quantum engineering of microscopic systems. These techniques require full control of all physical degrees of freedom with long coherence times. In comparison to well-established single-ion trapping methods (1–4), a similar level of control of neutral atoms has yet to be achieved because of their weaker interactions with external electromagnetic fields.

Thermal sources of neutral atoms, such as atomic beams, provide a flux of uncorrelated atoms with random arrival times. However, there is great interest in a source that would deliver a desired number of cold atoms at a time set by the experimentalist. Micromaser experiments, for example, use a dilute atomic beam, which results in a mean number of atoms inside the resonator that is much less than 1. Poissonian statistics, however, dictate that the probability of having more than one atom inside the res-

onator simultaneously does not vanish; this can easily destroy the ideal one-atom-maser operation (5). Another possible application is the controlled generation of single optical photons triggered by atoms entering a resonator with mirrors of ultrahigh reflectivity (a “high-finesse” resonator) one by one (6, 7). Other experiments require the placement of more than one atom into the region of interest. Quantum logic gates (8) can be implemented by entangling (2, 4, 9, 10) neutral atoms through their simultaneous coupling to the optical field of a resonator (11, 12). This is possible with the current technology, but in recent experiments (13, 14) atoms enter the cavity in a random way, rendering it impossible to have a certain small number of atoms on demand.

In comparison, our technique guarantees control of the position of individual neutral atoms with submicrometer precision. A standing-wave dipole trap is used to store any desired small number of cold atoms in a laser field interference pattern, localizing the trapped atoms to better than half of the optical wavelength. Changing the laser pa-

rameters moves this interference pattern along with the trapped atom in a prescribed way. Whereas the transportation of atomic clouds has recently been realized using magnetic potentials (15), here we demonstrate the controlled transport of a single atom.

Optical dipole traps (16–21) are based on the interaction between an electric component of the light field  $\mathbf{E}$  and the induced atomic electric dipole moment  $\mathbf{d}$ , which is proportional to  $\mathbf{E}$ . The interaction energy  $U = -\langle \mathbf{d} \cdot \mathbf{E} \rangle / 2$  is proportional to the local light intensity. If the laser frequency is smaller than the atomic resonance frequency, the atom is attracted to the region of maximum intensity. Thus, the simplest optical dipole trap is a focused laser beam. Tuning the laser frequency far away from all atomic resonances substantially reduces the photon scattering rate, and the atom is trapped in a nearly conservative potential. In contrast, a magneto-optical trap (MOT) (22) provides dissipative forces and serves as a convenient source of single cold atoms (23, 24). Atoms captured from the background gas interact with the near-resonant light field of the MOT and scatter photons from the laser beams. This fluorescence signal monitors the number of trapped atoms in real time (Fig. 1). These atoms can be transferred into a dipole trap superimposed on the MOT without any loss, thus allowing us to experiment with a predetermined number of atoms (24).

Our dipole trap consists of two counter-propagating laser beams with equal intensities and optical frequencies  $\nu_1$  and  $\nu_2$ , producing a position-dependent dipole potential  $U(z, t) = U_0 \cos^2[\pi(\Delta\nu t - 2z/\lambda)]$ , where  $U_0$  is the local trap depth,  $z$  is the position of the atoms,  $\lambda = 1064$  nm is the optical wavelength ( $\lambda = c/\nu_1 \approx c/\nu_2$ , where

Institut für Angewandte Physik, Universität Bonn, Wegelerstrasse 8, D-53115 Bonn, Germany.

\*To whom correspondence should be addressed. E-mail: kuhr@iap.uni-bonn.de

## REPORTS

$c$  is the speed of light), and  $\Delta\nu = \nu_1 - \nu_2 \ll \nu_1, \nu_2$ . An atom initially trapped in the stationary standing wave ( $\Delta\nu = 0$ ) is moved along the optical axis by changing the frequency difference  $\Delta\nu$ , which causes the potential wells to move at a velocity  $v = \lambda\Delta\nu/2$ . The value of  $\Delta\nu$  is controlled with two acousto-optic modulators (AOMs) (Fig. 2). A similar technique is used in (25, 26) to accelerate atomic ensembles in optical lattices. In our case, both dipole trap laser beams, which are derived from a Nd:YAG (yttrium-aluminum-garnet) laser, are focused to a waist of  $w_0 = 30 \mu\text{m}$ . With a total power of 5 W, these two beams produce a maximum trap depth of  $U_{\text{max}}/k_B \approx 2 \text{ mK}$  (where  $k_B$  is the Boltzmann constant). Because the typical kinetic energy of a trapped atom ( $\sim 0.1 \text{ mK}$ ) is considerably smaller than the trap depth, the radial localization ( $\sim 7 \mu\text{m}$ ) is much tighter than the waist  $w_0$ . For these parameters, the maximum photon scattering rate is about  $3 \text{ s}^{-1}$  and can be neglected on the relevant time scales. On the basis of our previous experiment (24), we expect a spin relaxation time on the order of half a minute.

Our device allows us to accelerate a single trapped cesium atom and bring it to a stop at preselected points along the standing wave. For this purpose, a digital frequency synthesizer sweeps the frequency of one of the modulators in a phase-continuous way. We control the transportation distance with submicrometer precision by heterodyning both frequencies of the AOM drivers. A counter monitors the number of cycles during a frequency sweep, which directly measures the transportation distance in multiples of  $\lambda/2$ .

We use position-sensitive fluorescence detection (27) to detect a displaced atom within the dipole trap. The atom is illuminated by a weak resonant probe laser ( $\lambda_{\text{res}} = 852 \text{ nm}$ ,  $F = 4 \rightarrow F' = 5$  transition of the  $D_2$  line) overlapped with a repumping laser ( $F = 3 \rightarrow F' = 4$ ), providing cyclic optical excitation. The resulting fluorescence signal is detected by a second optical system identical to the one used for collecting fluorescence from the MOT (Fig. 3A). A high-precision linear motion stage displaces both detector and imaging optics to the exact transportation distance. Spatial filters limit the fluorescence detection to a field of view of radius  $\sim 40 \mu\text{m}$ . This is much smaller than the typical displacements, which are on the order of several millimeters. Resonant illumination yields a burst of up to 100 fluorescence photons in 50 ms at near zero background, which warrants secure detection of the atom at its new position (Fig. 3B). The fixed imaging optics permanently monitor the MOT region, both to verify the presence of a single atom

and to confirm the disappearance of the displaced atom from the MOT.

This detection scheme serves to prove the deterministic delivery of a single atom to a desired spot. The measured probability of observing the transported atom as a function of the displacement (Fig. 4, circles) shows that for small distances, the fraction of detected atoms is above 90%. However, the position dependence of the trap depth limits the detection efficiency for larger displacements  $z$  from the laser focus. The tight focusing of the trapping

laser beams yields a Rayleigh length  $z_0$  of only 3 mm. Because of the divergence of the Gaussian trapping beams, the local trap depth  $U_0$  scales with the displacement  $z$  from the focus as  $U_0(z) = U_{\text{max}}(1 + z^2/z_0^2)^{-1}$ . During resonant excitation, the atom is heated by scattering photons. The fluorescence signal lasts until the atom is evaporated out of the trap, which happens on average after  $N = 2mU_0(z)/p_{\text{ph}}^2$  scattering events, where  $m$  is the atomic mass and  $p_{\text{ph}} = h/\lambda_{\text{res}}$  (where  $h$  is Planck's constant) is the photon momentum. As a conse-

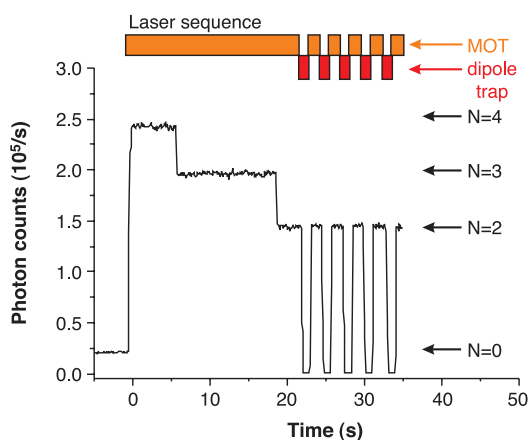


**Fig. 1.** Loading the dipole trap with a desired number of atoms. Fluorescence from the MOT shows discrete signal levels and directly monitors the number of trapped atoms  $N$ . Here, the MOT is switched on at  $t = 0$  and four atoms are captured from the background gas. A desired number of atoms (two, in this case) is transferred into the dipole trap by turning on the dipole trap laser a few milliseconds before the MOT lasers are turned off. After 1 s, the reverse procedure recaptures the atoms into the MOT, showing the same fluorescence level (i.e., the same number of atoms) as before. Transfer of atoms between the two traps can be repeated many times without losing atoms.

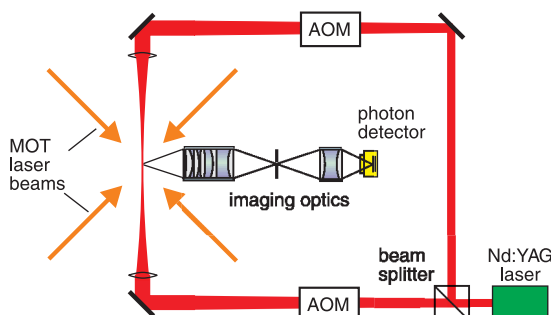


**Fig. 2.** The MOT and dipole trap are overlapped in the center of a vacuum cell (not shown). AOMs are used to control the frequencies of the two laser beams that form the dipole trap. Fluorescence light is collected by imaging optics with spatial filtering apertures and is detected by a single photon counting detector. The photon count rate from the MOT is  $5 \times 10^4 \text{ s}^{-1}$  per atom (see Fig. 1).

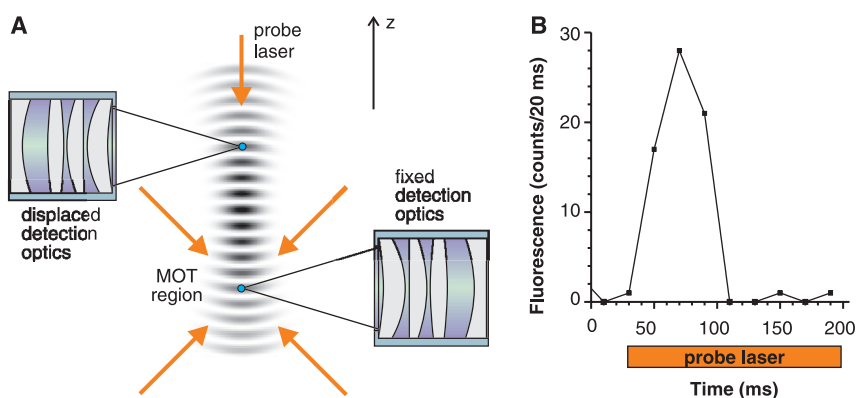


**Fig. 3.** "Single-atom conveyor belt." (A) Moving the interference pattern transfers a trapped atom from the MOT region to a new position where the resonance fluorescence is collected by the displaced detection optics. (B) Detection of a single atom in the dipole trap. The graph shows a burst of fluorescence photons from one atom in the dipole trap displaced by  $500 \mu\text{m}$ . The probe laser is switched on with a time delay of 30 ms after transportation and produces no measurable contribution to stray light.

quence, the fluorescence signal decreases for larger distances.

Nonetheless, the transportation efficiency is much higher than shown by the resonant illumination detection. As the atom moves away from the laser focus during the transportation procedure, the depth of the dipole potential decreases. This potential flattening is sufficiently slow to result in adiabatic cooling of the transported atom. Simple calculations show that even for relatively hot atoms with a kinetic energy of half the maximum trap depth, the transportation distance should be on the order of 5 mm. To prove this, we have used the MOT to detect the atom with 100% efficiency. Without resonant illumination, the displaced atom is transported back to  $z = 0$  before we switch on the MOT lasers to reveal the presence or absence of the atom. The results of this measurement (Fig. 4, squares) reveal that even for distances as large as 10 mm, the two-way transportation efficiency remains above 80%.

The investigation of various accelerations at a constant displacement of 1 mm yields a constant transportation efficiency of more than 95% until the acceleration exceeds a value of  $10^5$  m/s<sup>2</sup>. At larger accelerations, the efficiency rapidly decreases as a result of the reduction of the dipole trap laser power, caused by the finite bandwidth of the AOMs. An acceleration of  $10^5$  m/s<sup>2</sup> allows us to change the atomic velocity from 0 to 10 m/s in 100  $\mu$ s.

In all the manipulations described above, the dipole trap is never switched off. However, it is of interest to see whether the atomic position and velocity can still be determined after a period of zero interaction with light fields. Using the conveyor belt as a catapult and the MOT as a target, we realized a rudimentary linear accelerator for a single atom. Initially, a single atom is displaced by 3 mm, which is substantially larger than the capture region (about 300  $\mu$ m) of our high-field gradient MOT (24). We now move the standing wave in the opposite direction, accelerating the atom

back over 0.5 mm. The atom is now released into free flight 2.5 mm away from the MOT by rapidly switching off the standing wave. In the absence of light, it then flies with a final velocity of 2 m/s toward the position of the MOT. Note that the initial kinetic energy of the trapped atom limits the precision of this velocity (to about 5% in this case). The time of flight can still be calculated with enough accuracy such that if the MOT lasers are turned on exactly at this time, the atom is always recaptured by the MOT, demonstrating the working principle of the catapult. We observed, however, that the MOT is not a perfectly defined target. Slight misalignment of the MOT laser beams causes unbalanced resonant light forces to deflect the atom from its path before dissipative forces capture it in the center of the trap. This effect reduces the recapture efficiency to 20% if we direct the atom into the operating MOT. This capture rate is due to pure magnetic trapping only, as has been confirmed by measuring the same capture efficiency of 20% without accelerating the atom toward the MOT. More generally, a dipole trap made of crossed laser beams could eject an atom into a direction different from the beam axis. This ability to deliver a single atom with a well-defined velocity and direction of motion could trigger further experiments in which single atoms act as a probe for various physical systems.

The single-atom conveyor belt can transport a desired number of atoms into a resonator of high finesse in order to implement basic quantum gate operations (8, 11, 12). Although the standing-wave structure has a periodicity of  $\lambda/2$ , the absolute control of the axial position of the atoms in the dipole trap is currently limited by the size of the MOT (less than 20  $\mu$ m). Lowering this limit and consecutively loading single atoms from the MOT into the dipole trap should generate a string of atoms with well-defined separations to create an "atomic shift register." The standing-wave structure

also provides tight confinement of trapped atoms, leading to axial oscillation frequencies of about 400 kHz. This opens a route to the application of Raman sideband cooling techniques (28) and the generation of non-classical motional states of atoms (29). Additional cooling of the atoms will improve the performance of the conveyor belt with respect to both transportation efficiency and atomic localization. Spin relaxation times of many seconds, in combination with the state-selective detection at the level of a single neutral atom (24), show that this system promises to be a versatile tool for future experiments with full control of internal and external atomic degrees of freedom.

References and Notes

1. W. Neuhauser, M. Hohenstatt, P. E. Toschek, H. Dehmelt, *Phys. Rev. A* **22**, 1137 (1980).
2. Q. A. Turchette *et al.*, *Phys. Rev. Lett.* **81**, 3631 (1998).
3. C. Roos *et al.*, *Phys. Rev. Lett.* **83**, 4713 (1999).
4. C. A. Sackett *et al.*, *Nature* **404**, 256 (2000).
5. E. Wehner, R. Seno, N. Sterpi, B.-G. Englert, H. Walther, *Opt. Commun.* **110**, 655 (1994).
6. C. K. Law, H. J. Kimble, *J. Mod. Opt.* **44**, 2067 (1997).
7. M. Hennrich, T. Legero, A. Kuhn, G. Rempe, *Phys. Rev. Lett.* **85**, 4872 (2000).
8. H.-K. Lo, S. Popescu, T. Spiller, Eds., *Introduction to Quantum Computation and Information* (World Scientific, Singapore, 1998).
9. E. Hagle *et al.*, *Phys. Rev. Lett.* **79**, 1 (1997).
10. A. Rauschenbeutel *et al.*, *Science* **288**, 2024 (2000).
11. T. Pellizzari, S. A. Gardiner, J. I. Cirac, P. Zoller, *Phys. Rev. Lett.* **75**, 3788 (1995).
12. A. Beige, D. Braun, B. Tregenna, P. L. Knight, *Phys. Rev. Lett.* **85**, 1762 (2000).
13. C. J. Hood, T. W. Lynn, A. C. Doherty, A. S. Parkins, H. J. Kimble, *Science* **287**, 1447 (2000).
14. P. W. H. Pinkse, T. Fischer, P. Maunz, G. Rempe, *Nature* **404**, 365 (2000).
15. W. Hänsel, J. Reichel, P. Hommelhoff, T. W. Hänsch, *Phys. Rev. Lett.* **86**, 608 (2001).
16. A. Ashkin, *Phys. Rev. Lett.* **24**, 156 (1970).
17. S. Chu, J. E. Bjorkholm, A. Ashkin, A. Cable, *Phys. Rev. Lett.* **57**, 314 (1986).
18. S. Chu, *Science* **253**, 861 (1991).
19. H. J. Metcalf, P. van der Straten, *Laser Cooling and Trapping* (Springer, New York, 1999).
20. V. I. Balykin, V. G. Minogin, V. S. Letokhov, *Rep. Prog. Phys.* **63**, 1429 (2000).
21. R. Grimm, M. Weidemüller, Y. B. Ovchinnikov, *Adv. At. Mol. Opt. Phys.* **42**, 95 (2000).
22. E. L. Raab, M. Prentiss, A. Cable, S. Chu, D. E. Pritchard, *Phys. Rev. Lett.* **59**, 2631 (1987).
23. Z. Hu, H. J. Kimble, *Opt. Lett.* **19**, 1888 (1994).
24. D. Frese *et al.*, *Phys. Rev. Lett.* **85**, 3777 (2000).
25. M. Ben Dahan, E. Peik, J. Reichel, Y. Castin, C. Salomon, *Phys. Rev. Lett.* **76**, 4508 (1996).
26. S. R. Wilkinson, C. F. Bharucha, K. W. Madison, Q. Niu, M. G. Raizen, *Phys. Rev. Lett.* **76**, 4512 (1996).
27. We first reported the direct observation of an individual cesium atom in a standing-wave optical dipole trap in D. Meschede *et al.*, *Light and Matter: Interaction at the Microscopic Level* (presented at the Quantum Theory Centenary Symposia, Berlin, 12 December 2000).
28. S. Hamann *et al.*, *Phys. Rev. Lett.* **80**, 4149 (1998).
29. M. Morinaga, I. Bouchoule, J.-C. Karam, C. Salomon, *Phys. Rev. Lett.* **83**, 4037 (1999).
30. Supported by the Deutsche Forschungsgemeinschaft and the state of Nordrhein-Westfalen.

21 May 2001; accepted 5 June 2001  
 Published online 14 June 2001;  
 10.1126/science.1062725  
 Include this information when citing this paper.

**Fig. 4.** Deterministic delivery of a single atom, as shown by the probability of detecting a displaced atom as a function of the displacement. Each data point results from  $\sim 100$  shots performed with one atom each. Circles: The atom is detected by resonant illumination at its new position. Squares: More efficient detection by moving the atom back and recapturing it into the MOT.

